

In situ generation of antibacterial bimetallic silver and copper nanocomposites using *Tinospora cordifolia* leaf extract as bio reductant

Venkata Ramanamurthy Gollapudi ¹, Umamahesh Mallavarapu ^{2,*}, Jaswanth Seetha ^{2,3},
Varaprasad Duddela ⁴, Venkateswara Rao Amara ³, Chandra Sekhar Vatti ⁵, Varadarajulu
Anumakonda ⁶

¹Department of Chemistry, V. R College, Nellore, Andhra Pradesh, India

²Department of Chemistry, Rajeev Gandhi Memorial College of Engineering & Technology, Nandyal, Andhra Pradesh, India

³Research scholar, Department of Chemistry, JNTUA, Anantapur, Andhra Pradesh, India

³Research scholar, Department of Environmental science, Yogi Vemana University, Kadapa, Andhra Pradesh, India

⁴Department of Mechanical Engineering, Rajeev Gandhi Memorial College of Engineering & Technology, Nandyal, Andhra Pradesh, India

⁵Centre for Composite Materials, International Research Center, Kalasalingam University, Krishnan Koil, Tamilnadu, India

*corresponding author e-mail address: mahesh1962rgm@gmail.com | Scopus ID [57204242722](https://orcid.org/0000-0002-5720-4272)

ABSTRACT

The method of *in situ* generation was employed to produce binary silver and copper bimetallic nanocomposites (BNCFs) using lesser emission pollutant biological plant species i.e., *Tinospora cordifolia* (TC) leaf broth as reducing agent. The generated BNCFs were confirmed by different spectrophotometric studies i.e. Fourier Transform Infrared (FTIR), Scanning Electron Microscope (SEM) along with Energy Dispersive X-ray (EDX), X-ray Diffractometer (XRD), Primary and Secondary thermogravimetric (TG & DTG) analysis and Differential Scanning Calorimetry (DSC). The bio synthesized nanocomposite cotton fabrics (NCFs) were found to be spherical in shape and with an average size of 80nm from SEM analysis. The elements silver and copper were confirmed by observing peaks at 3keV and 1keV, respectively, from EDX spectra. The XRD studies revealed the crystalline nature of BNCFs. TG and DTG analysis explained the catalytic activity of silver and copper with lesser thermal stability. The BNCFs showed good tensile properties, using universal testing machine. The BNCFs also exhibited good antibacterial activity against disease producing G^{+ve} and G^{-ve} bacteria. The BNCFs may be considered to make bandage cloths, napkins etc., in the medical field.

Keywords: *TC leaf extract; Nanocomposite cotton fabrics; silver and copper bimetallic nanoparticles; Mechanical properties; In situ generation; Antibacterial activity.*

1. INTRODUCTION

Many researchers have been attracted towards biological reduction processes to produce metal nanoparticles (MNPs), metal oxide nanoparticles due to their lesser toxicity emission into environment, easy and simple methodology, available abundantly, biocompatibility and genuine applicability in medicine [1-5]. The *in situ* generation method was adopted by many researchers to minimize agglomeration and inferior properties while preparing MNPs in polymer matrices [6]. A few researchers utilized plant species constituents for the *in situ* generation of MNPs such as copper nanoparticles (CuNPs) and silver nanoparticles (AgNPs) [7-9]. Recently, the bimetallic nanoparticles (BMNPs) were synthesized owing to their improved properties, variety of applications and synergy with a provision to change their molar ratio than individual monometallic nanoparticles (MNPs) [10,11]. BMNPs are showing more technological advantages than their individual counterpart MNPs due to improved properties in electronics, catalysis and optics [12,13]. A few reports are available in the literature for the synthesis of BMNPs utilizing plant parts species by bioreduction method [14-17]. *Tinospora cordifolia* (TC) is found to be one of the most divine plants of ayurvedic medicine and commonly known as Guduchi and Tippateega in southern areas of India [18]. The TC plant species parts were found to be useful and extensively employed to cure a number of diseases and disorders of human beings. The TC plant

releases anxiety, stress and illness by acting as adaptogen potent and increases the resistance of human body. The TC leaf extract mixed with *Ocimum sanctum* (Tulasi) utilized as a medicine for curing dengue patients to increase the immunity and platelet count. Alleviate allergies, high fever gout arthritis, rheumatic disorders of inflammation, chronic skin disorders i.e. psoriasis-eczema were cured, reduce the side effects of chemotherapy drugs and control of blood glucose levels, TC plant, employed as a medicinal plant. It is also used as a health supplement due to its anti-oxidant properties and capability to support the liver and immune system. Guduchi acted as an antiangiogenic [19-23]. TC plant species parts are employed in various medical applications. Hence, the authors in the present work employed aqueous TC leaf broth as a reductant for the generation of BNCFs. The BNCFs were confirmed by FTIR, SEM, XRD and EDX. The thermal stability and catalytic effect were studied, utilizing TG-DTG studies. Universal testing machine (UTM) and disc diffusion method were performed to test mechanical strength and antimicrobial activity of BNCFs. These NCFs were considered to make antibacterial napkins, bandage cloths etc. in medicine, agriculture as target pesticides and packing applications.

2. MATERIALS AND METHODS

2.1. Materials.

Fresh leaves of TC plant, white fabric, Nutrient Agar (AR), $\text{CuSO}_4 \cdot 5\text{H}_2\text{O}$ (AR) and AgNO_3 (AR) (Sigma Aldrich) were utilized in the present research work.

2.2. Aqueous TC leaf extract.

The TC plant leaves were confirmed by consulting a botanist before preparing the extract. The TC leaves were plucked from the plant before sunrise. The picked TC leaves washed the number of times with conductivity water until all the adhered soil contaminants, dust particles and if any other impurities were removed. The cleaned leaves were dried in the sunlight and chopped into pieces. 100g of chopped leaves were poured into 900 mL of distilled water present in a glass vessel. It is heated at 80°C for 20min on a thermally controlled magnetic stirrer with 200rpm rotating speed. The aqueous leaf extract turned into pale yellowish green. For obtaining a clear leaf extract solution, the contents in glass vessel were centrifuged and filtered. The obtained TC leaf extract was stored in reagent bottles and placed at 4°C in the coolers until it was used.

2.3. Preparation of the matrix.

The cellulose cotton fabric was rinsed in water and washed to remove adhered starch impurity. The dried white cotton fabric was cut into pieces of 80mm x 270mm. 200mL of prepared TC leaf extract was taken in 250mL beaker and each piece was dipped in it. The beaker was then placed on a magnetic stirrer at laboratory temperature and subjected to a constant stirring with a speed of 200rpm for 24 h. The color of white cotton cloth was changed to pale green due to TC leaf extract got diffused into it. These pieces are known as matrices. The matrix was further washed a number of times to remove unadhered organic and other impurities of the leaf extract present on it. The matrices were dried and preserved in desiccators until tested.

2.4. Generation of BNCFs.

AgNO_3 and $\text{CuSO}_4 \cdot 5\text{H}_2\text{O}$ Aqueous source solutions (1-5mM) were made using earlier standard procedures and taken separately in 250mL beakers. Different aliquots mixture concentrations source solutions with a total concentration of 5mM (4+1mM, 3+2mM, 2.5+2.5mM, 2+3mM and 1+4mM AgNO_3 and $\text{CuSO}_4 \cdot 5\text{H}_2\text{O}$) were prepared and taken in individual beakers. Each piece of matrix was dipped in 250mL beakers with different concentrations of aliquots of source solutions. These beakers containing source solutions were placed on a magnetic stirrer and stirred at 200rpm for 24h. It was covered with tin foil to overcome

catalytic oxidation of silver at laboratory conditions. For comparison, 5mM individual source solutions of AgNO_3 and $\text{CuSO}_4 \cdot 5\text{H}_2\text{O}$ were utilized for the generation of MNPs (AgNPs and CuNPs) with a similar procedure on NCFs. The pale yellow greenish color matrix was changed to a color between brown and greenish brown owing to the generation of BMNPs on NCFs. The BNCFs and individual MNCFs were removed and washed a number of times to remove unadhered source solutions and it was dried. The *in situ* generated BMNPs on NCFs were initially confirms with the color change.

2.5. Characterization.

The BNCFs with instantaneous generation of AgNPs and CuNPs were analyzed by different spectral characteristics such as XRD, FTIR, SEM and TGA. The tensile and antibacterial properties were also tested. The SEM with EDX spectra of BNCFs were recorded using JEOL JSM-IT500 scanning electron microscope (Akishima, Tokyo, Japan) operated at 10 kV. The Smart Tiff software of the microscope was employed to determine the size of BMNPs. FTIR (BRUKER ALPHA-II, Billerica, MA · USA) spectrophotometer was employed to record the spectra in the range of 4000 cm^{-1} to 400 cm^{-1} wavenumber with 32 scans at a resolution of 4 cm^{-1} . RIGAKU MINI FLEX-600 XRD was employed to know the crystalline nature of BNCFs and matrix. The diffractograms were recorded at $2\theta = 10^\circ$ to 80° at a scanning rate of $4^\circ/\text{min}$. Perkin Elmer TGA-7 thermogravimetric analyzer (Akron, Ohio, United States) was utilized to record the primary and derivative thermograms employing the heating rate of $10^\circ\text{C}/\text{min}$ to know the thermal stability and catalytic activity of BMNPs. The thermograms of DSC were obtained using PERKINELMER-STA600 analyzer (Westborough, MA, United States). The antibacterial killing activity of BNCFs [24] was tested using standard disc method against pathogenic bacteria *S. aureus* (AATCC 6538) and *K. pneumonia* (AATCC 147) with AATCC 100 standard test. Image J software was utilized to calculate the diameter of the zone of killing of pathogenic bacteria. The tensile properties of BNCFs were tested with INSTRON-3369 Universal testing machine (Norwood, MA 02062-2643, USA) as per ASTM D 638 specifications. The BNCFs were cut into rectangular pieces with dimensions of 150 mm length and 10 mm width and employed in the present study with a gauge length of 50 mm by conducting at an extension rate of 5 mm/min using 5 specimens for each sample and their average values are given.

3. RESULTS

3.1. Physical visual identification of BNCFs.

The instantaneously generated AgNPs and CuNPs on NCFs were confirmed initially with persistent color change by physical visual observation. The BNCFs made utilizing equimolar aliquot mixtures of $\text{CuSO}_4 \cdot 5\text{H}_2\text{O}$ and AgNO_3 source solutions (2.5mM + 2.5mM) concentrations, 5mM individual MNPs and for comparison matrix and cotton fabric were photographed and presented and the obtained digital images were shown in Fig. 1a-e. During the formation of matrix, the white color changed to pale yellow green (Fig. 1b). The individual MNPs (AgNPs and CuNPs)

were changed to brown (Fig. 1c) and bluish brown ((Fig. 1d), respectively.

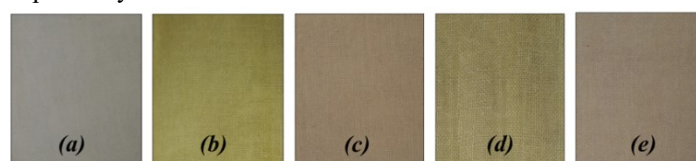


Figure 1. Digital photographs of (a) white cloth; (b) matrix; MNCFs (c) AgNPs (5mM); (d) CuNPs (5mM); (e) BNCFs (2.5mM Ag+ 2.5mM Cu).

However, the BNCFs obtained with equimolar solution of AgNO₃ and CuSO₄.5H₂O appeared as light bluish brown (Fig. 1e). The BNCFs using different aliquots of source solutions remained unaffected in their color even after several washings with conductivity water. The *in situ* generation of BMNPs on NCFs was preliminarily confirmed with visual change of color between the matrix and the BNCFs.

3.2. SEM with EDX.

The SEM studies were investigated to confirm the generation of BMNPs in NCFs. The recorded SEM images of BNCFs and individual MNCFs are presented in Fig. 2a, Fig. 2b and Fig. 2c, respectively. The shape of generated BMNPs and MNPs on NCFs in all the three cases was globular. In the case of MNPs it can be noticed from Fig. 2a and Fig. 2b, the individually generated AgNPs and CuNPs were found to be in moderate number. However, a large number of BMNPs in NCFs were generated (Fig. 2c). Silver and copper elements present in MNCFs and BNCFs were confirmed by EDX spectra is given in Fig. 2a^I-c^I. An energy band peak was observed at 3keV and 1keV for individual MNPs (AgNPs and CuNPs). The BMNPs on NCFs were also exhibited similar peaks at 3keV and 1keV. The similar peaks were also observed by earlier researchers [25]. The other reported EDX spectra energy band peaks for copper at 8keV and 9keV were not found in the present work due to the use of lower concentration of CuSO₄.5H₂O source solution and reveals the generation of BMNPs on NCFs. The size distribution of generated MNPs and BMNPs was presented in the form of histograms as shown in Fig. 2a^{II}- c^{II}. The average size of BMNPs was in the range of 20-180 nm with a mean size of 80 nm. But the size of individual MNPs were found to be 90 nm and 120 nm for AgNPs and CuNPs, respectively. However, BNCFs exhibited reduced particle size as compared to those with MNPs.

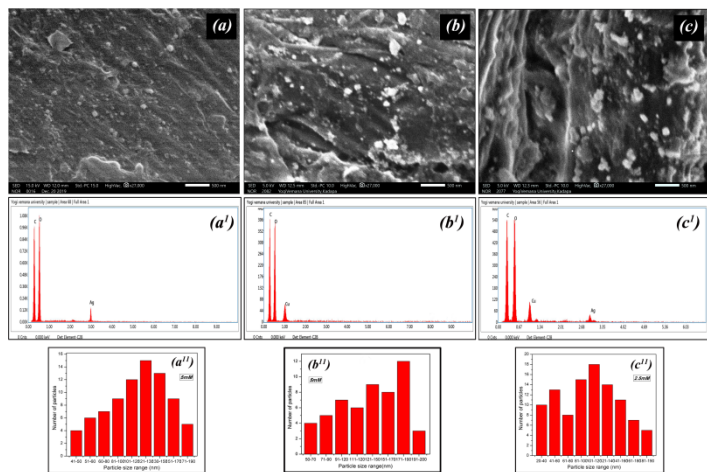


Figure 2. SEM photographs of NCFs made with (a) AgNPs, (b) CuNPs (5mM) and (c) BNCFs (2.5mM + 2.5mM); EDX spectra of NCFs (a^I) AgNPs, (b^I) CuNPs and (c^I) BNCFs; Histograms of NCFs (a^{II}) AgNPs, (b^{II}) CuNPs and (c^{II}) BNCFs.

3.3. FTIR studies.

The molecular entities present in TC leaf extract which are responsible for the formation of BMNPs and MNPs in NCFs were analyzed by FTIR spectral studies. The Fig. 3 represents the recorded FTIR spectra of individual MNPs (AgNPs and CuNPs) and BMNPs on NCFs, white cloth and matrix. The FTIR spectra of white cloth and matrix are presented in Fig. 3 indicating that both matrix and white cloth contain similar functional groups. The

spectra of individual MNPs and corresponding BMNPs on NCFs are also presented in Fig. 3. It is also observed from Fig. 3 that the matrix exhibited a high intensity of the peak than that of cotton fabric. It is because of some molecular functionalities are diffused into cellulose cotton fabric. However, the FTIR spectra of BMNPs and MNPs generated on NCFs by *in situ* method also showed the same absorption peaks as observed in the case of matrix. The BMNPs showed an absorption band at 3279cm⁻¹ corresponding to -OH functionality as in alkaloids, flavonoids, glycosides, steroids and poly alcohols present in TC leaf extract [26]. The other absorption bands at 2878cm⁻¹, 1637cm⁻¹, 1327cm⁻¹ and 1008cm⁻¹ were due to C-H stretching vibrations of alkanes, C=O stretching vibration of fatty acids, carboxylic O-H bending vibration of fatty acids and C-O and C-O-C stretching vibrations, respectively [27]. Further, it is also observed that the intensity of absorption peak exhibited by BNCFs was lower than that of matrix at 3279cm⁻¹, indicating the involvement of -OH functional group of TC leaf extract in the bio reduction of bimetallic ions (Ag⁺ and Cu²⁺) into metallic silver and copper (Ag⁰ and Cu⁰) nanoparticles. The generated BMNPs and MNPs in NCFs was further confirmed with bioreduction. The shift of absorption peaks towards lower frequencies (Fig. 3) of BMNPs as compared with absorption peaks of MNPs owing to generation of large number of BMNPs in NCFs with a little agglomeration.

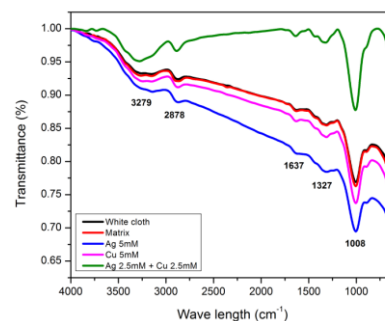


Figure 3. FTIR Spectra of white cloth, Matrix, MNCFs and BNCFs

3.4. XRD spectral studies.

To study the effect of crystallinity of MNCFs and BNCFs, the XRD spectral study was carried and the obtained X-ray diffractograms of BNCFs, MNCFs and matrix are presented in Fig. 4a. Both matrix and white cloth exhibited similar bands with the planes which are overlapping with each other (not shown in Figure) at 15.04° (101), 16.71° (10-1), 22.92° (002) and 34.41° (040) related to cellulose -I structure [28]. The intensity of the individual MNCFs was found to be higher than the matrix. However, the BMNPs generated on NCFs exhibited higher and lower intensity than the matrix and individual MNCFs, respectively. The higher peak intensity of BNCFs indicates an increase in crystallinity, but lesser than individual MNPs. It is due to the utilization of lower concentrations of CuSO₄.5H₂O source solutions to produce a lesser number of CuNPs with slight agglomeration. The X-Ray diffractograms of generated MNPs and BMNPs as shown in Fig. 4a have not clear peaks for visualization. In order to see them clearly, the diffractogram of the BNCF (2.5mM + 2.5mM) was highlighted in 2θ = 30°–80° range (Fig. 4b). The XRD peaks at 38.84° (111), 46.91° (200), 64.75° (220) and 77.89° (311) and other peaks 44.26° (111), 51.26° (200) and 70.99° (220) were related to AgNPs and CuNPs, respectively.

[10,29]. But, MNPs generated on NCFs exhibited higher intensity peaks of AgNPs as compared with CuNPs. The formation of BMNPs in NCFs was further confirmed by observing XRD analysis.

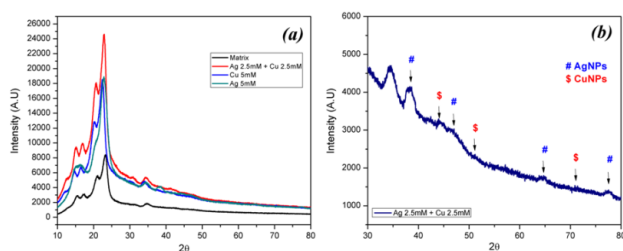


Figure 4. XRD spectra of (a) Matrix, MNCFs and BNCFs; (b) Expanded diffractogram of BNCF ($2\theta=30^{\circ}$ – 80°).

3.5. TG-DTG & DSC analysis.

Thermogravimetric analysis was carried to test whether the produced MNPs and BMNPs on NCFs exhibit thermal stability or not. The recorded primary and secondary thermograms of individual MNPs and BMNPs generated on NCFs are presented in Fig. 5a and Fig. 5b. The thermograms of DSC were given in Fig. 5c. Both MNCFs and BNCFs exhibited two stages of thermal degradation. The initial phase of deterioration was started at temperature range of 43 °C and ended at 180 °C. This type of degradation was owing to the evaporation of moisture content and the volatile constituents of the NCFs and matrix. From Fig. 5a, the other step of degradation was initiated and ended in the case of matrix at 310 °C and completed at 416 °C, respectively. However, the MNPs and BMNPs formed on NCFs exhibited the degradation temperatures started at 284 °C and 276 °C and ended at 398 °C and 377 °C, respectively. But, the NCFs with generated BMNPs showed lesser thermal stability than the matrix indicating that BMNPs in NCFs and individual MNPs in NCFs exhibited catalytic activity to increase the thermal degradation [30,31]. The behavior of two stages of thermal degradation and exothermic reaction were confirmed by the secondary thermogravimetric and DSC studies, respectively.

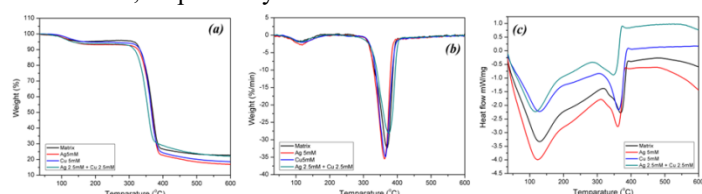


Figure 5. (a) TG analysis, (b) DTG analysis and (c) DSC analysis of NCFs with MNPs and BNPs.

3.6. Mechanical properties.

The tensile properties [32,33] of individual MNCFs and BNCFs were tested to make thermally stable and high strength BNCFs. The computed tensile parameters and obtained stress strain curves are shown in Fig. 6 and are presented in Table 1. The tensile stress and percentage of strain for white cotton fabric and matrix were given as 16.65 MPa and 17.52 MPa and 0.23% and 0.23%, respectively as shown in Fig.6 and Table 1. The matrix exhibited higher values than the white cloth due to the diffusion of leaf extract. The tensile stress and percentage of strain for individual AgNPs and CuNPs on NCFs and BMNPs on NCFs were found to be 22.59 MPa and 0.23 %, 21.46 MPa and 0.21 %, 27.61 MPa and 0.19 %, respectively. An increase in the tensile strength and decrease the percentage of strain was observed in

both cases i.e., individual MNCFs and BMNCFs. The BMNPs on NCFs exhibited the highest tensile stress and the modulus value was also high as compared with white fabric and the matrix. However, the BNCFs exhibited lower modulus value than individual MNPs.

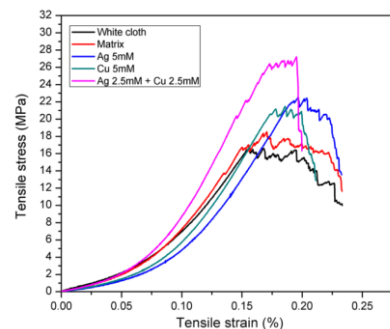


Figure 6. Tensile properties of white cloth, MNCFs, BNCFs and Matrix.

3.7. Action on disease producing pathogenic bacteria.

One of the important applications of MNCFs in medical field is antibacterial property. Hence, the authors tested the microbial activity of synthesized BMNPs on NCFs (2.5mM + 2.5mM), individual MNCFs (5mM) by the disc method against *S. aureus* and *K. pneumonia* disease producing bacteria. The zones of clearance obtained for both bacteria by individual MNCFs, BNCFs and matrix were photographed and the obtained digital images were presented in Fig.7a and Fig. 7b, respectively. The diameters of zone of inhibition were measured and the values are presented in Table 2. The matrix does not show any zone of inhibition indicating that it does not exhibit antibacterial property. While the NCFs exhibited their outstanding antibacterial activity due to the formation of clear zones than MNPs. The measured values of zone of inhibition are in comparison with other researcher's work [34].

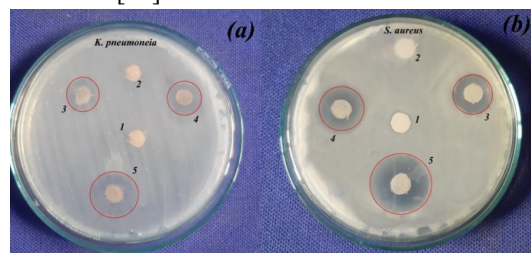


Figure 7. Photographs of antimicrobial activity by MNCFs and BNCFs against (a) *K. pneumonia* (b) *S. aureus*.

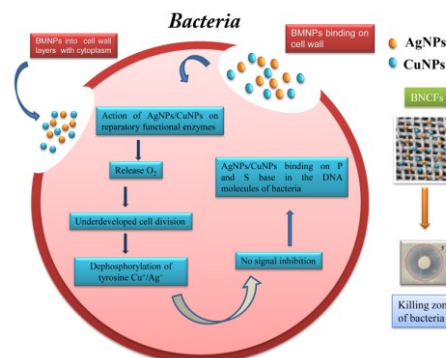


Figure 8. Action mechanism of BMNPs on pathogenic bacteria

Jaswanth *et al.*, observed a similar behavior in case of BMNPs (Ag and Cu) synthesized by bioreduction method [11]. Hence, the NCFs with BMNPs possessing good mechanical and antibacterial activity and can be utilized in medical applications

such as beds and pillows in hospitals, for wound dressing, antibacterial bandage cloths and also as napkins.

3.8. Mechanism of antibacterial activity of BMNPs on pathogenic bacteria.

A possible general mechanism of killing of pathogenic bacteria by BMNPs was presented in Fig. 8. It can be inferred from Fig. 8 that both AgNPs and CuNPs on NCFs can adhere to cell wall of bacteria. The respiratory enzymes in bacterial cells are

in contact with BMNPs and inhibit several functions in the cell and cause damage to the cells [35]. As a result, there will be a generation of reactive oxygen species, which are produced possibly through the inhibition of a respiratory enzyme by both silver ions and copper ions and attack the cell. BMNPs may bind on soft base Phosphorus (P) and Sulfur (S) in the DNA molecule of bacteria.

Table 1. Induced tensile stress-strain values of NCCFs, white cloth and matrix at maximum loads

Type of cloth	Tensile Strain (%)	Tensile Stress (MPa)	Young's Modulus (MPa)	Maximum Load (N)
White cloth	0.23	16.65	189.11	91.56
Matrix	0.23	17.52	190.85	101.85
Ag 5mM	0.23	22.59	214.35	129.89
Cu 5mM	0.21	21.46	233.38	150.21
Ag 2.5mM + Cu 2.5mM	0.19	27.61	289.12	196.82

Table 2. Antibacterial Zone of inhibition exhibited by NCCFs vs *K. pneumoniae* and *S. aureus*

Sample with label	Diameter of clear zone (mm)	
	<i>K. pneumoniae</i>	<i>S. aureus</i>
White cloth (1)	0	0
Matrix (2)	0	0
Cu 5mM (3)	16	17
Ag 5mM (4)	16	18
Ag 2.5mM + Cu 2.5mM(5)	21	22

4. CONCLUSIONS

The *in situ* generated BMNPs on NCFs were generated using aqueous *Tinospora cordifolia* leaves broth as reducing agent. The bio synthesized BNCFs and for comparison, MNCFs were analyzed by different spectral characteristics such as SEM, FTIR, XRD and TGA. The antibacterial activity and tensile were also studied. The molecular functionalities of TC leaf broth are responsible for bioreduction and to obtain both BMNPs and MNPs on NCFs were confirmed by FTIR spectral studies. The average size of the calculated BMNPs by SEM analysis was found to be

with an average size of 80nm. The presence of elemental metallic copper and silver was confirmed by EDX spectra. The peaks obtained from XRD spectrum revealed the formation of both AgNPs and CuNPs in NCFs. The BNCFs exhibited good tensile and antibacterial properties. The NCFs formed with BMNPs by *in situ* method can be used in medical field for making antibacterial bandage cloths, napkins etc. and further can also be employed in photocatalytic reactions.

5. REFERENCES

- Espenti, C.S.; Rao, K.K.; Rao, K. M. Bio-synthesis and characterization of silver nanoparticles using Terminalia chebula leaf extract and evaluation of its antimicrobial potential. *Mat. Lett* **2016**, *174*, 129-133. <https://doi.org/10.1016/j.matlet.2016.03.106>
- Amara, V.R.; Basa, A.; Mallavarapu, U.M.; Vatti, C.; Gopireddy, S.V.; Anumakonda, V. Preparation and properties of cotton nanocomposite fabrics with in situ generated copper nanoparticles using Red sanders powder extract as a reducing agent. *Inorg. Nano-Metal Chem* **2019**, *49*, 1-6. <https://doi.org/10.1080/24701556.2019.1661437>.
- Surendra, T.V.; Roopan, S.M. Photocatalytic and antibacterial properties of phytosynthesized CeO₂ NPs using Moringa oleifera peel extract. *J. of Photochem. Photobiol. B: Biol* **2016**, *161*, 122-128. <https://doi.org/10.1016/j.jphotobiol.2016.05.019>.
- Ganesh, E.; Roopan, S.M. Green synthesis, spectroscopic investigation and photocatalytic activity of lead nanoparticles. *Spectro. Act. Part A: Molec. Biomol. Spectr* **2015**, *139*, 367-373. <https://doi.org/10.1016/j.saa.2014.12.066>.
- Birusanti, A.B.; Mallavarapu, U.; Nayakanti, D.; Espenti, C.S.; Mala, S. Sustainable green synthesis of silver nanoparticles by using Rangoon creeper leaves extract and their spectral analysis and anti-bacterial studies. *IET nanobiotech* **2018**, *13*, 71-76. <https://doi.org/10.1049/iet-nbt.2018.5117>.
- He, J.; Kunitake, T.; Nakao, A. Facile in situ synthesis of noble metal nanoparticles in porous cellulose fibers. *Chem. Mat* **2003**, *15*, 4401-4406. <https://doi.org/10.1021/cm034720r>.
- Rao, A.V.; Ashok, B.; Umamahesh, M.; Chandrasekhar, V.; Subbareddy, G.V.; Rajulu, A.V. Preparation and properties of silver nanocomposite fabrics with in situ-generated silver nanoparticles using red sanders powder extract as reducing agent. *Int. J. Polym. Anal. Charact* **2018**, *23*, 493-501. <https://doi.org/10.1080/1023666X.2018.1485200>.
- Sadanand, V.; Tian, H.; Varada, R.A.; Satyanarayana, B. Antibacterial Cotton Fabric with In Situ Generated Silver Nanoparticles by One Step Hydrothermal Method. *Int. J. Polym. Anal. Charact* **2017**, *22*, 275-279. <https://doi.org/10.1080/1023666X.2017.1287828>.
- Pusphalatha, R.; Ashok, B.; Hariram, N.; Rajulu, A.V. Nanocomposite polyester fabrics with in situ generated silver nanoparticles using tamarind leaf extract reducing agent. *Int. J. Polym. Anal. Charact* **2019**, *24*, 1-9. <https://doi.org/10.1080/1023666X.2019.1614265>.
- Venkateswara, R.A.; Ashok, B.; Uma, M.M.; Venkata, S.G.; Chandra, S.V.; Venkata, R.G.; Varada, R.A. Antibacterial cotton fabrics with in situ generated silver and copper bimetallic nanoparticles using red sanders powder extract as reducing agent. *Int. J. Polym. Anal. Charact* **2019**, *24*, 346-354. <https://doi.org/10.1080/1023666X.2019.1598631>.

11. Seetha, J.; Mallavarapu, U.M.; Akepogu, P.; Mesa, A.; Gollapudi, V.R.; Natarajan, H.; Anumakonda, V.R. Biosynthesis and study of bimetallic copper and silver nanoparticles on cellulose cotton fabrics using Moringa oliefera leaf extraction as reductant. *Inorg. Nano-Met. Chem.* **2020**, *1-8*, <https://doi.org/10.1080/24701556.2020.1725571>.

12. Hasanzadeh, M.; Shadjou, N. Electrochemical and photoelectrochemical nano-immunesensing using origami paper based method. *Mat. Sci. Eng: C* **2016**, *61*, 979-1001, <https://doi.org/10.1016/j.msec.2015.12.031>.

13. Dang-Bao, T.; Pla, D.; Favier, I.; Gómez, M. Bimetallic nanoparticles in alternative solvents for catalytic purposes. *Catalysts* **2017**, *7*, <https://doi.org/10.3390/catal7070207>.

14. Mamatha, G.; Varada Rajulu, A.; Madhukar, K. In situ generation of bimetallic nanoparticles in cotton fabric using aloe vera leaf extract, as a reducing agent. *J. Nat. Fib* **2018**, *1-9*, <https://doi.org/10.1080/15440478.2018.1558146>.

15. Hassabo, A.G.; El-Naggar, M.E.; Mohamed, A.L.; Hebeish, A.A. Development of multifunctional modified cotton fabric with tri-component nanoparticles of silver, copper and zinc oxide. *Carbohydr. polym* **2019**, *210*, 144-156, <https://doi.org/10.1016/j.carbpol.2019.01.066>.

16. Xia, B.; He, F.; Li, L. Preparation of bimetallic nanoparticles using a facile green synthesis method and their application. *Langmuir* **2013**, *29*, 4901-4907, <https://doi.org/10.1021/la400355u>.

17. Smuleac, V.; Varma, R.; Sikdar, S.; Bhattacharyya, D. Green synthesis of Fe and Fe/Pd bimetallic nanoparticles in membranes for reductive degradation of chlorinated organics. *J. membr. Sci.* **2011**, *379*, 131-137, <https://doi.org/10.1016/j.memsci.2011.05.054>.

18. Singh, S.S.; Pandey, S.C.; Srivastava, S.; Gupta, V.S.; Patro, B.; Ghosh, A.C. Chemistry and medicinal properties of *Tinospora cordifolia* (Guduchi). *Ind J Pharma* **2003**, *35*, 83-91.

19. Sinha, K.; Mishra, N.P.; Singh, J.; Khanuja, S.P.S. *Tinosporacordifolia* (Guduchi), a reservoir plant for therapeutic applications: A Review. *Indian journal of traditional knowledge* **2004**, *3*, 257-270.

20. Shefali, C.; Nilofer, S. Gaduchi-The Best Ayurvedic Herb. *Pharma Innov* **2013**, *2*, 97.

21. Choudhary, N.; Siddiqui, M.B; Azmat, S.; Khatoon, S. *Tinosporacordifolia*: ethnobotany, phytopharmacology and phytochemistry aspects. *Int. J. Pharma. Sci. Res* **2013**, *4*, 891-897, [http://dx.doi.org/10.13040/IJPSR.0975-8232.4\(3\).891-99](http://dx.doi.org/10.13040/IJPSR.0975-8232.4(3).891-99).

22. Saha, S.; Ghosh, S. *Tinosporacordifolia*: One plant, many roles. *AncSci Life* **2012**, *31*, 151-155, <https://doi.org/10.4103/0257-7941.107344>.

23. Sharma, V.; Pandey, D. Beneficial effects of *Tinosporacordifolia* on blood profiles in male mice exposed to lead. *ToxiInt* **2010**, *17*, 8-11.

24. Gopinath, K.; Kumaraguru, S.; Bhakayaraj, K.; Mohan, S.; Venkatesh, K.S.; Esakkirajan, M.; Kaleeswarran, P.; Alharbi, N.S.; Kadaikunnan, S.; Govindarajan, M.; Benelli, G. Green synthesis of silver, gold and silver/gold bimetallic nanoparticles

using the *Gloriosasuperba* leaf extract and their antibacterial and antibiofilm activities. *Micro. Pathogen.* **2016**, *101*, 1-11, <https://doi.org/10.1016/j.micpath.2016.10.011>.

25. Wu, W.; Lei, M.; Yang, S.; Zhou, L.; Liu, L.; Xiao, X.; Jiang, C.; Roy, V.A. A one-pot route to the synthesis of alloyed Cu/Ag bimetallic nanoparticles with different mass ratios for catalytic reduction of 4-nitrophenol. *J. Mat. Chem. A* **2015**, *3*, 3450-3455, <https://doi.org/10.1039/C4TA06567K>.

26. Reddy, N.M.; Reddy, R.N. *Tinosporacordifolia* chemical constituents and medicinal properties: a review. *Sch Acad J Pharm* **2015**, *4*, 364-369.

27. Padma, M.; Govindh, B.; Rao, B.V. Synthesis & Characterization of Fluorescent Silver Nanoparticles stabilized by *TinosporaCordifolia* leaf Extract-A Green Procedure. *Int J Eng Res IndAppl* **2014**, *4*, 100-107.

28. Zhou, Q.; Lv, J.; Ren, Y.; Chen, J.; Gao, D.; Lu, Z.; Wang, C. A green in situ synthesis of silver nanoparticles on cotton fabrics using Aloe vera leaf extraction for durable ultraviolet protection and antibacterial activity. *Tex. Res. J* **2017**, *87*, 2407-2419, <https://doi.org/10.1177/0040517516671124>.

29. Ismail, M.; Khan, M.I.; Khan, S.A.; Qayum, M.; Khan, M.A.; Anwar, Y.; Akhtar, K.; Asiri, A.M.; Khan, S.B. Green synthesis of antibacterial bimetallic Ag-Cu nanoparticles for catalytic reduction of persistent organic pollutants. *J. Mat. Sci.: Mat. Electr* **2018**, *29*, 20840-20855, <https://doi.org/10.1007/s10854-018-0227-2>.

30. Sadanand, V.; Tian, H.; VaradaRajulu, A.; Satyanarayana, B. Antibacterial Cotton Fabric with In Situ Generated SilverNanoparticles by One Step Hydrothermal Method. *Int. J.Polym. Anal. Charact*, **2017**, *22*, 275-279, <https://doi.org/10.1080/1023666X.2017.1287828>.

31. Kishanji, M.; Mamatha, G.; Obi Reddy, K.;Varada, R.A.; Madhukar, K. In situ generation of silver nanoparticles in cellulose matrix using *Azadirachtaindica* leaf extract as a reducing agent. *Int. J.Polym. Anal.Charact* **2017**, *22*, 734-740, <https://doi.org/10.1080/1023666X.2017.1369612>.

32. Perelshtein, I.; Applerot, G.; Perkas, N.; Guibert, G.; Mikhailov, S.; Gedanken, A. Sonochemical coating of silver nanoparticles on textile fabrics (nylon, polyester and cotton) and their antibacterial activity. *Nanotech* **2008**, *19*, 245705, <https://doi.org/10.1088/0957-4484/19/24/245705>.

33. Sedighi, A.; Montazer, M.; Hemmatinejad, N. Copper nanoparticles on bleached cotton fabric: in situ synthesis and characterization. *Cellulose* **2014**, *21*, 2119-2132, <https://doi.org/10.1007/s10570-014-0215-5>.

34. Valodkar, M.; Modi, S.; Pal, A.; Thakore, S. Synthesis and anti-bacterial activity of Cu, Ag and Cu-Ag alloy nanoparticles: a green approach. *Mat. Res. Bullet* **2011**, *46*, 384-389, <https://doi.org/10.1016/j.materresbull.2010.12.001>.

35. Prabhu, S.; Poulouse, E.K. Silver nanoparticles: mechanism of antimicrobial action, synthesis, medical applications, and toxicity effects. *Int nano lett.* **2012**, *2*, <https://doi.org/10.1186/2228-5326-2-32>.

6. ACKNOWLEDGEMENTS

We express our sincere thanks to the department and authorities, RGM CET, Nandyal, for providing needful requirements.



© 2020 by the authors. This article is an open access article distributed under the terms and conditions of the Creative Commons Attribution (CC BY) license (<http://creativecommons.org/licenses/by/4.0/>).